



Engineering *Mesorhizobium loti* pyridoxamine–pyruvate aminotransferase for production of pyridoxamine with L-glutamate as an amino donor

Yu Yoshikane^a, Asuka Tamura^a, Nana Yokochi^a, Khalil Ellouze^a, Eitora Yamamura^b, Hanae Mizunaga^b, Noboru Fujimoto^b, Keiji Sakamoto^b, Yoshihiro Sawa^c, Toshiharu Yagi^{a,*}

^a Faculty of Agriculture and Agricultural Science Program, Graduate School of Integrated Arts and Sciences, Kochi University, Monobe-Otsu 200, Nankoku, Kochi 783-8502, Japan

^b Technical Department, Daiichi Fine Chemical Co., Ltd., 530 Chokeiji, Takaoka, Toyama 933-8511, Japan

^c Department of Life Science and Biotechnology, Shimane University, Matsue, Shimane 690-8504, Japan

ARTICLE INFO

Article history:

Received 31 May 2010

Received in revised form 24 July 2010

Accepted 26 July 2010

Available online 1 August 2010

Keywords:

Pyridoxamine

Pyridoxamine–pyruvate aminotransferase

Substrate specificity

Rational design

Random mutagenesis

ABSTRACT

Pyridoxamine–pyruvate aminotransferase (PPAT), a novel pyridoxal 5′-phosphate-independent aminotransferase, reversibly catalyzes the transfer of an amino group between pyridoxamine and pyruvate to generate pyridoxal and L-alanine. The enzyme can be used for synthesis of pyridoxamine, a promising candidate for prophylaxis and treatment of diabetic complications. A disadvantage of PPAT for industrial application to the synthesis is that it requires an expensive amino acid L-alanine as an amino donor. Here, mutated PPATs with a high activity toward 2-oxoglutarate (and hence toward L-glutamate) were prepared by a rational design plus random mutagenesis of the wild-type PPAT because L-glutamate is readily and economically available. The PPAT(Y35H/V70R/F247C) showed 9.1-fold lower K_m and 4.3-fold higher k_{cat} values than those of the wild-type PPAT. The model of the complex of mutated PPAT and pyridoxyl-L-glutamate showed that γ -carboxyl group of L-glutamate was hydrogen-bound with an imidazole group of His35. The production of pyridoxamine from pyridoxal with transformed *Escherichia coli* cells expressing the mutated PPAT did not correlate with the k_{cat} value or catalytic efficiency of the mutated PPAT but with K_m value at a low level. *E. coli* cells expressing the PPAT(M2T/Y35H/V70K/E212G) could be used for in vitro conversion of pyridoxal into pyridoxamine at 30 °C with L-glutamate as an amino donor.

© 2010 Elsevier B.V. All rights reserved.

1. Introduction

Vitamin B₆ consists of 6 natural forms, pyridoxamine, pyridoxal, pyridoxine, pyridoxamine 5′-phosphate, pyridoxal 5′-phosphate (PLP), and pyridoxine 5′-phosphate. PLP serves as a cofactor of many reactions involved in amino acid metabolism, such as transamination, racemization, decarboxylation, and deamination [1]. Recently, addition to this cofactor action, vitamin B₆ and its derivatives have been shown to be effective antioxidants and quenchers of singlet oxygen [2–6]. Furthermore, pyridoxamine interferes with the formation of advanced glycation end-products (AGEs) and advanced lipoxidation end-products (ALEs), and thus inhibits the non-enzymatic modification of proteins. AGEs and ALEs are the major pathogenic factors in diabetic complications [7,8]. In an ani-

mal model, pyridoxamine indeed inhibits early renal disease and dyslipidemia in the streptozotocin-diabetic rats [9]. Phase 2 studies of patients with type 1 and type 2 diabetes and overt nephropathy showed that pyridoxamine provided for a foundation for further evaluation of AGE inhibitor in diabetic nephropathy [10]. Thus, pyridoxamine is a promising candidate for a prophylactic and/or a remedy for diabetic complications. The amount of consumption of pyridoxamine should become massive because it has been estimated that there are about 180 million diabetics in the world.

Pyridoxamine is currently synthesized by chemical methods. Two routes (oxidative or non-oxidative method) for the chemical synthesis are known, where the starting material is the readily and economically available pyridoxine. The oxidative method, which has been used for industrial production, changes pyridoxine to pyridoxal, and then pyridoxal to pyridoxamine through the pyridoxal oxime, which is reduced with Pd/C catalyst to pyridoxamine [11]. The non-oxidative one changes pyridoxine to pyridoxamine by the Gabriel synthesis [12]. Although the latter method does not use Pd/C catalyst, it takes several steps including production of a primary alkyl halide derivative of pyridoxine. Enzymatic or microbial synthetic method is generally preferable in the environmental and energetic aspects, if they are available. As far as we know, no enzymatic method for production of pyridoxamine has been reported.

Abbreviations: PPAT, pyridoxamine–pyruvate aminotransferase; PLP, pyridoxal 5′-phosphate; IPTG, isopropyl- β -D-thiogalactopyranoside; X-gal, 5-bromo-4-chloro-3-indolyl- β -D-galactopyranoside; AGEs, advanced glycation end-products; ALEs, advanced lipoxidation end-products; CHES, N-cyclohexyl-2-aminoethanesulfonic acid.

* Corresponding author. Tel.: +81 88 864 5191; fax: +81 88 864 5191.

E-mail address: yagito@kochi-u.ac.jp (T. Yagi).

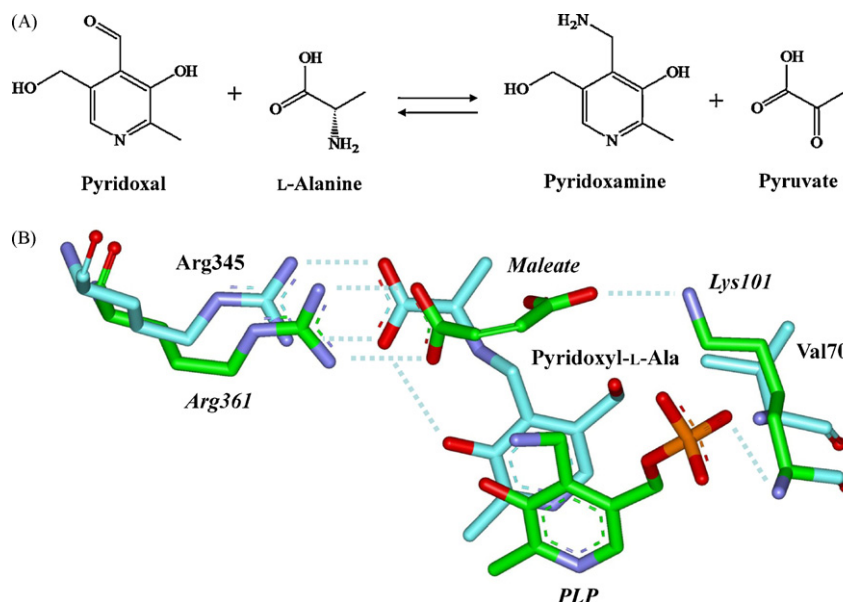


Fig. 1. (A) Reaction catalyzed by pyridoxamine–pyruvate aminotransferase. (B) Superimposition of active site residues found in PPAT–pyridoxyl-L-alanine complex (C–C bonds are shown in a cyan color, PDF code, 2Z9X) and *Thermus thermophilus* aspartate aminotransferase–maleate complex (C–C bonds are shown in a green color, 1BKG). Amino acid residues in the latter are shown in italics. The figures were drawn with WebLab. (For interpretation of the references to color in this figure legend, the reader is referred to the web version of the article.)

Recently, we have identified the gene encoding pyridoxamine–pyruvate aminotransferase (PPAT) in a nitrogen-fixing symbiotic bacterium, *Mesorhizobium loti* MAFF303099, characterized the over-expressed recombinant enzyme [13], and determined its tertiary structure [14]. PPAT shows high catalytic efficiency and thermal stability, and reversibly catalyzes the transfer of an amino group between pyridoxamine and pyruvate to produce pyridoxal and L-alanine (Fig. 1A). Thus, PPAT may be used for an industrial enzymatic production of pyridoxamine if its activity toward L-glutamate, which is much cheaper than L-alanine, could be increased to use L-glutamate as an amino donor.

PPAT is classified into class V aminotransferases of fold type I of the PLP-dependent enzymes even though it is not PLP-dependent [13]. A representative enzyme in the fold type I is aspartate aminotransferase which shows activity towards L-glutamate. Thus, a comparison of the active site architecture of PPAT to that of aspartate aminotransferase will give us a rational design of mutated PPAT with a high activity towards L-glutamate. Fig. 1B shows superimposed active site residues of PPAT binding pyridoxyl-L-alanine (PDB code, 2Z9X) and *Thermus thermophilus* aspartate aminotransferase binding maleate (1BKG). In aspartate aminotransferase, one carboxylate in L-glutamate analog, maleate, is hydrogen-bonded to Lys101 and the other forms charged hydrogen bonds with Arg361. Arg361 of aspartate aminotransferase corresponds to Arg345 of PPAT and binds to α -carboxyl group of substrates. Lys101 in aspartate aminotransferase binds to γ -carboxyl group of substrate L-glutamate. In PPAT, the corresponding amino acid residue is Val70. Thus, if Val70 is changed to basic amino acid residue, PPAT may show reactivity towards L-glutamate.

Here, PPAT was engineered to increase reactivity toward L-glutamate or 2-oxoglutarate by the rational design plus random mutagenesis; because PPAT catalyzes reversible reaction as shown in Fig. 1A, the enzyme with higher activity toward L-glutamate should show high reactivity toward the corresponding amino receptor 2-oxoglutarate. The transformed *Escherichia coli* cells expressing PPAT(M2T/Y35H/V70K/E212G) could convert pyridoxal into pyridoxamine in a yield of almost 100%.

2. Materials and methods

2.1. Bacterial strains, cultivation, plasmids, and reagents

E. coli strains, JM109 and BL21(DE3), were purchased from TaKaRa Bio (Tokyo, Japan) and Novagen-Merck Japan (Tokyo, Japan), respectively. *E. coli* cells were cultured in a modified LB medium (1% polypeptone, 0.5% yeast extract, and 1% NaCl) containing 50 μ g/ml ampicillin at 37 °C. Plasmids, pET6806 carrying wild-type PPAT gene [13], pET21a (Novagen-Merck Japan), pUC119 (TaKaRa Bio), and pQE-30 (QIAGEN Japan, Tokyo, Japan), were used. *M. loti* MAFF303099, which has the PPAT gene, was obtained from MAFF (Ministry of Agriculture, Forestry and Fisheries) DNA bank (Tsukuba, Japan). Plasmids carrying various mutated PPATs were prepared in this study and are available on request. Pyridoxal and pyridoxamine were purchased from Wako (Tokyo, Japan) and Tokyo Chemical Industry (Tokyo, Japan), respectively. Sodium pyruvate, L-alanine, and L-glutamate were purchased from Wako. Potassium 2-oxoglutarate and lysozyme from chicken egg white were purchased from Sigma Japan (Tokyo, Japan).

2.2. Site-directed mutagenesis and expression of mutated PPAT

Genes encoding PPAT mutants were prepared with the plasmid pET6806 as a template, as described previously [13]. The primers used were: for PPAT(V70K), 5'-GCGAGCCGAAGCTCGGCC-3' and 5'-GGCCGAGCTTCGGCTCGC-3'; for PPAT(V70R), 5'-GCGAGCCGAGGCTCGGCC-3' and 5'-GGCCGAGCCTCGGCTCGC-3'. The underlined letters indicate mismatched sites. Presence of the desired mutation and the absence of other mutation in the mutated enzyme genes were confirmed by the DNA sequencing with an ABI PRISM 3100-Avant Genetic Analyzer (Applied Biosystems Japan, Tokyo, Japan). The constructed plasmids containing the mutated PPAT genes were introduced into BL21(DE3) cells, and then the transformed cells were aerobically grown in 5 ml of LB medium containing ampicillin at 37 °C for 16 h. The cells were harvested by centrifugation at 8400 \times g for 10 min at 4 °C, and then washed with 0.9% NaCl, and stored at –20 °C until use.

2.3. First error-prone PCR for preparation of PPAT(Y35H/V70K) and PPAT(V70R/F247C)

Random mutagenesis of an *mlr6806* (PPAT) gene was performed by the error-prone PCR. The BamHI–EcoRI fragment of pET6806(V70K) carrying the V70K-mutated PPAT gene was inserted into the BamHI/EcoRI sites of pUC119 to construct pUC6806(V70K). The pUC6806(V70K) was used as a template for error-prone PCR. Error-prone PCR was performed in a reaction mixture (50 μ l) consisting of GC buffer (TaKaRa Bio), 2 ng pUC6806(V70K), 0.2 mM dNTPs, 4 mM MgCl₂, 20 pmol each primer, and 2.5 units BIOTAQ™ DNA polymerase (BIOLINE, London, England). Primers, 5'-CCCGGATCCGAGCTGATGTACTCGCAGCAT-3' and 5'-CCCGAATTCTCAGGCGTCCGCGTTCGATTACG-3', with a BamHI site (underlined in the former) and an EcoRI site (underlined in the latter), respectively, were used. The PCR conditions were: heating at 94 °C for 2 min; 50 cycles at 94 °C for 15 s, 57.5 °C for 30 s, and 72 °C for 180 s.

2.4. Screening of clones expressing mutated PPAT with a high activity toward 2-oxoglutarate

The randomly mutated PCR fragments were subjected to 1% agarose gel electrophoresis, and purified with an E. Z. N. A. Gel Extraction Kit (Omega Bio-Tek, Norcross, GA, USA). Isolated DNA fragments were digested with BamHI and EcoRI, and then ligated into the BamHI/EcoRI sites of pUC119 treated with alkaline phosphatase. The plasmids harboring the isolated DNA fragments were introduced into JM109 competent cells, and then the cells were grown on LB agar plates containing ampicillin, 0.1 mM isopropyl- β -D-thiogalactopyranoside (IPTG), and 40 μ g/ml 5-bromo-4-chloro-3-indolyl- β -D-galactopyranoside (X-gal). White colonies on the plate were picked up, and each was inoculated into a separate well containing 0.9 ml of LB-ampicillin in a deep 96-well plate (BIO-BIK, Tokyo, Japan). The plate was incubated at 37 °C for 16 h under shaking, and then centrifuged at 1200 \times g for 10 min at 4 °C. The precipitated cells in a deep 96-well plate were suspended in 55 μ l of 10 mM Tris–HCl (pH 7.0) containing 0.1 mg/ml lysozyme. The cell suspensions were incubated for 1 h at 37 °C to lyse the cells. Supernatants (50 μ l each) obtained by centrifugation at 1200 \times g for 10 min at 4 °C were separately transferred to a well of another 96-well plate. The enzyme reaction in each well was done for 2 h at 30 °C by the addition of 150 μ l of reaction mixture consisting of 50 mM Tris–HCl, pH 9.0, 1 mM pyridoxamine, and 50 mM 2-oxoglutarate (or 5 mM sodium pyruvate). Then, absorbance at 405 nm of a Schiff base between the produced pyridoxal and Tris base of the reaction mixture in each well was measured with a Bio-Rad Model 550 microplate reader (Tokyo, Japan). Two clones expressing a mutated PPAT with a higher activity toward 2-oxoglutarate than that of PPAT(V70K) were selected. Plasmids were prepared from the selected clones, and then the mutated base was determined by DNA sequencing. PPAT(Y35H/V70K) and PPAT(V70R/F247C) were consequently obtained.

2.5. Screening of clones expressing mutated PPATs which produce a high amount of pyridoxamine with L-glutamate as an amino donor

Plasmid pUC6806, pUC6806(V70K), or pUC6806(Y35H/V70K) was used for PCR as a template together with primers 5'-ATGATGCGCTATCCCGAATGCGG-3' and 5'-TCAGGCGTCGGCGTTCGATTAC-3'. The amplified DNA fragments were inserted into SmaI site of a plasmid pQE-30 to prepare pQE6806, pQE6806(V70K), or pQE6806(Y35H/V70K). Second error-prone PCR with the pQE plasmids as a template, and pQE-sequencing primer set (QIAGEN) as primers were done by

essentially the same method as that described above. The DNA fragments were digested with BamHI and PstI, and then ligated into the BamHI/PstI sites of pQE-30. The plasmids were introduced into JM109 cells, and then the cells were grown on LB agar plates containing ampicillin. The colonies on the plate were picked up, and each was inoculated into LB medium containing ampicillin and 1 mM IPTG, then the production of pyridoxamine with L-glutamate as an amino donor was measured as described later. Two clones, which showed a higher production of pyridoxamine than PPAT(V70K)-expressing cells, were selected, and then the plasmids in the cells were sequenced. The plasmids expressed PPAT(V70K/E212G) and PPAT(M2T/V70K).

2.6. Construction of PPATs mutated at three or four sites

For preparation of PPAT(Y35H/V70R/F247C), site-specific mutagenesis of Tyr35 to His was performed with a KOD-Plus-Mutagenesis kit (Toyobo, Tokyo, Japan) according to the instruction manual. Primers, 5'-CATGATTACGATCCCTGCATCCAGCTCC-3' (the underlining indicates mismatched sites) and 5'-AAGCACCGTACGGCCGAGGCC-3', and a template, pUC6806(V70R/F247C), were used. PPAT(Y35H/V70R/F247C) was expressed by pUC6806(Y35H/V70R/F247C) in JM109 cells. pQE6806(M2T/V70K/E212G) which expressed PPAT(M2T/V70K/E212G) in JM109 were prepared by a PCR in which pQE6806(V70K/E212G), 5'-TCAGGCGTCGGCGTTCGATTAC-3' and 5'-ATGACGCGCTATCCCGAATGCGG-3' were used as a template and primers, respectively. The amplified DNA fragment was then inserted into SmaI site of pQE-30. Similarly, PCR was done with pQE6806(Y35H/V70K) as a template. The amplified DNA fragment was inserted into SmaI site of pQE-30 to prepare pQE6806(M2T/Y35H/V70K), which expressed PPAT(M2T/Y35H/V70K) in JM109. To prepare pQE6806(M2T/Y35H/V70K/E212G), which expressed PPAT(M2T/Y35H/V70K/E212G) in JM109, pQE6806(M2T/Y35H/V70K) and pQE(V70K/E212G) were separately digested with XhoI, and applied to an agarose gel electrophoresis. Then, the DNA fragment with 0.5 kbp from the former and that with 4.1 kbp from the latter were ligated. The ligated DNA fragment was inserted into pQE-30. The presence of mutation at the desired site and absence of other mutations was confirmed by DNA sequencing with an ABI PRISM 3100-Avant Genetic Analyzer.

2.7. Preparation of crude extracts containing mutated PPATs and their purification

The crude extracts were prepared as described previously [13], and mutated PPATs were purified essentially by the same procedure as that for purification of the wild-type PPAT [14]. Briefly, the cells expressing the mutated PPATs were suspended in 0.5 ml of 20 mM potassium phosphate, pH 8.0, containing 1 mM EDTA and 1 mM phenylmethylsulfonyl fluoride. The cell suspension was sonicated twice for 15 s on ice, and then centrifuged at 8400 \times g for 20 min at 4 °C. The supernatants obtained were used as crude extracts. For the purification of mutated PPATs, crude extracts were sequentially applied to a butyl-Toyopearl, QA52, and Sephacryl S-200 column chromatographies.

2.8. Enzyme and protein assays

Pyridoxamine-2-oxoglutarate aminotransferase activity was determined by the phenylhydrazine method as follows. The reaction mixture (0.4 ml) consisted of 0.1 M borate–KOH (pH 9.0), 50 mM 2-oxoglutarate, 3 mM pyridoxamine, and the crude extract or the enzyme. The reaction was performed at 30 °C for 10–30 min and stopped by the addition of 66 μ l of 9 M sulfuric acid. The pyri-

doxal produced was quantified by the phenylhydrazine method [13].

The kinetics was done by measuring the initial velocity of the enzyme reaction based on an initial increase or decrease in A_{391} or A_{360} due to pyridoxal produced or consumed, respectively, at 30 °C in 1 ml of a reaction mixture consisting of 0.1 M CHES-KOH (pH 9.0). Kinetic parameters for 2-oxoglutarate and pyruvate with the purified enzyme were determined by varying the concentration of 2-oxoglutarate and pyruvate from 0 to 400 mM and from 0 to 20 mM, respectively, at a fixed pyridoxamine concentration (3 mM). Kinetic parameters for L-glutamate and L-alanine with the purified enzyme were determined by varying the concentration of L-glutamate and L-alanine from 0 to 400 mM and from 0 to 250 mM, respectively, at a fixed pyridoxal concentration (0.6 mM). Kinetic parameters were determined using a curve fitting software (Kaleida Graph) to fit the Michaelis–Menten equation with the Levenberg–Marquardt algorithm.

Protein concentration was measured by the dye-binding method with bovine serum albumin as the standard [15]. The protein concentration of the purified enzyme was determined by the molecular absorption coefficient at 280 nm based on the amino acid composition [16].

2.9. Synthesis of pyridoxamine with the recombinant *E. coli* cells expressing the mutated PPATs

In vitro synthesis of pyridoxamine with the *E. coli* JM109 cells was done in the reaction mixture (0.1 ml) consisting of 0.1 M sodium phosphate buffer, pH 7.0, 100 mM pyridoxal, 400 mM L-glutamate, and the *E. coli* cells (50 of A_{660}) at 30 °C for 48 h. The concentration of pyridoxal was at a saturated level. The produced pyridoxamine was determined by an isocratic reversed-phase HPLC as described previously [13]. The control reaction was done with the *E. coli* cells harboring pQE-30 and expressing no PPAT. The amount of pyridoxamine produced by the mutated PPATs was calculated by subtracting amount of pyridoxamine in the control reaction.

2.10. Simulation of binding of pyridoxyl-L-glutamate to PPAT(Y35H/V70R/F247C)

The tertiary structure of PPAT(Y35H/V70R/F247C) was deduced by the MOE Protein Structure Evaluation program (Chemical Computing Group, Montreal, QC, Canada). Docking simulation was performed for the crystal structure of wild-type PPAT complexed with pyridoxyl-L-glutamate (PDB code 2Z9X) with the MMFF94x force field distribution in the MOE 2008.1001 program with the Monte Carlo docking procedure of ASE-Dock 2005 (Ryoka System, Tokyo, Japan). In the simulation experiment, 11 solutions were generated. Solutions were ranked according to total interaction energy, and the best-matched solution was considered.

2.11. Other methods

The molecular mass of the recombinant enzymes was determined by a size-exclusion chromatography with a Cosmosil 5Diol-120-II HPLC column. The standard proteins were used as described previously [13].

3. Results and discussion

3.1. Mutated PPATs by the rational design

The purified V70K and V70R enzymes showed a single protein band on a SDS-PAGE gel, and their molecular weights were 41 kDa (Fig. 2A). The mutated enzymes eluted at the same retention time of the wild-type PPAT (154 kDa) on the size-exclusion

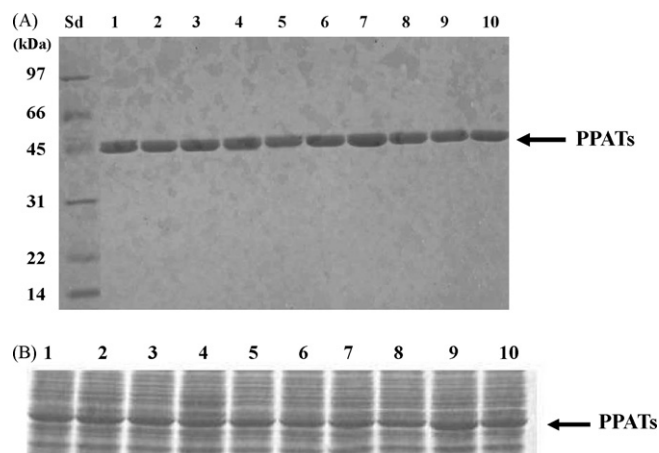


Fig. 2. (A) SDS-PAGE of some of purified mutated PPATs. Purified proteins (each 3 μ g) were applied: lane 1, V70K; 2, V70K/E212G; 3, wild-type; 4, M2T/V70K/E212G; 5, Y35H/V70K; 6, M2T/Y35H/V70K; 7, M2T/V70K; 8, M2T/Y35H/V70K/E212G; 9, V70R/F247C; and 10, Y35H/V70K/F247C. The standard proteins were applied to lane Sd. (B) Expression levels of wild-type and mutated PPATs. Crude extracts (10 μ g) from *E. coli* cells expressing the PPATs were applied as shown in (A).

chromatography, indicating that all mutated enzymes existed as a homotetramer. Thus, the mutations did not change the quaternary structure of PPAT. Table 1 shows kinetic parameters of the mutated PPATs. The V70K single mutation resulted in 1.7-fold increase in the catalytic efficiency (k_{cat}/K_m) for 2-oxoglutarate. The increase was caused by 2.2-fold increase in k_{cat} value. In contrast, the K_m value increased 1.3-fold, showing a slight decrease in the affinity for the substrate. The V70R mutation resulted in an inactivation of PPAT. Thus, V70K-mutated PPAT was used for an error-prone PCR to get mutated PPATs with a higher activity towards the substrates.

3.2. Mutated PPATs obtained by the error-prone PCR

The first error-prone PCR showed that 1–6 mutations occurred in the nucleotide sequence, corresponding to an average of 2 amino acid residue substitutions in the newly mutated PPATs. Out of about 1000 colonies expressing mutated PPATs, about 20 colonies, crude extracts of which showed higher activity of pyridoxamine–2-oxoglutarate aminotransferase, were selected at first. From them, two colonies were selected based on the specific activity and expression level of the mutated PPAT proteins, which was estimated from the densities on the SDS-PAGE gel. The genes of the mutated PPAT proteins encoded PPAT(Y35H/V70K) and PPAT(V70R/F247C). The mutated PPATs were expressed in JM109, and then purified homogeneously. They showed a single band of 41 kDa on SDS-PAGE, and had a molecular weight of homotetramers under native conditions. PPAT(Y35H/V70K) showed 10.2-fold higher reaction efficiency for 2-oxoglutarate than that of PPAT(V70K); K_m and k_{cat} values were 8.1-fold lower and 1.3-fold higher than those of PPAT(V70K), respectively (Table 1). PPAT(V70R/F247C) showed 3.7-fold higher reaction efficiency for 2-oxoglutarate than that of PPAT(V70K) although PPAT(V70R) showed no activity as described above. The result suggested that the substitution of Phe247 with Cys caused a proper adaptation of guanidino group with positive charge of Arg70 to interact with the γ -carboxyl group of L-glutamate.

The error-prone PCR with pQE6806(V70K) as the template, in which clones were selected based on the production of pyridoxamine by the intact cells expressing the mutated enzymes, gave another two mutated PPATs, PPAT(M2T/V70K) and PPAT(V70K/E212G). Interestingly, they showed only a slight

Table 1
Kinetic parameters of wild-type and mutant PPAT for 2-oxoglutarate and L-glutamate and production of pyridoxamine.

Enzyme	2-Oxoglutarate				L-Glutamate				Pyridoxamine produced (mM) ^a
	K_m (mM)	k_{cat} (s^{-1})	k_{cat}/K_m ($s^{-1} M^{-1}$)	Relative k_{cat}/K_m ^b	K_m (mM)	k_{cat} (s^{-1})	k_{cat}/K_m ($s^{-1} M^{-1}$)	Relative k_{cat}/K_m ^b	
Wild-type	80.1 ± 13.9	1.9 ± 0.1	23	1.0 (0.6)	123.4 ± 14.5	1.5 ± 0.1	12	1.0 (0.6)	8 ± 2.0
V70K	102.6 ± 9.1	4.1 ± 0.2	40	1.7 (1.0)	142.0 ± 22.3	2.7 ± 0.6	19	1.6 (1.0)	14 ± 0.6
V70R	ND	ND			ND	ND			NM
M2T/V70K	77.3 ± 12.2	3.9 ± 0.2	50	2.2 (1.3)	NM	NM			32 ± 0.6
Y35H/V70K	12.6 ± 1.1	5.2 ± 0.2	408	17.7 (10.2)	29.3 ± 5.4	2.9 ± 0.1	100	8.3 (5.3)	24 ± 0.6
V70K/E212G	110.3 ± 4.6	4.6 ± 0.1	42	1.8 (1.1)	NM	NM			23 ± 0.6
M2T/Y35H/V70K	21.1 ± 1.9	3.5 ± 0.1	167	7.3 (4.2)	44.2 ± 7.2	3.1 ± 0.6	70	5.8 (3.7)	40 ± 2.0
M2T/V70K/E212G	106.8 ± 18.5	4.6 ± 0.4	43	1.9 (1.1)	NM	NM			31 ± 0.6
M2T/Y35H/V70K/E212G	17.2 ± 1.1	4.0 ± 0.5	234	10.2 (5.9)	51.0 ± 5.0	3.0 ± 0.1	58	4.8 (3.1)	66 ± 4.5
V70R/F247C	61.3 ± 5.0	9.1 ± 0.3	148	6.4 (3.7)	133.5 ± 19.4	4.4 ± 0.3	33	2.8 (1.7)	24 ± 0.6
Y35H/V70R/F247C	8.8 ± 0.3	8.1 ± 0.2	916	39.8 (22.9)	42.4 ± 3.5	6.4 ± 0.2	152	12.7 (8.0)	27 ± 2.5

ND, not detectable; NM, not measured.

^a Concentration of pyridoxamine produced was calculated by subtraction of the value (30 mM) produced by a blank plasmid from that produced by the plasmid expressing the PPATs.

^b The numbers in the parenthesis indicate the value compared with that of V70K mutant.

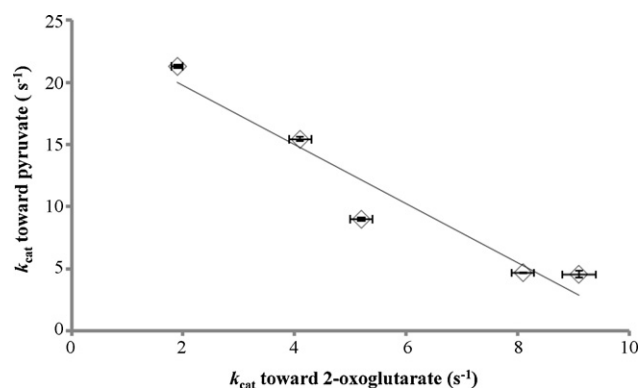


Fig. 3. Relationship between catalytic turnover numbers for 2-oxoglutarate and those for pyruvate determined for the wild-type and mutated PPATs. The linear regression line was drawn by Excel. The R value was -0.96 .

increase (1.3- and 1.1-folds, respectively) in the catalytic efficiency for 2-oxoglutarate (Table 1).

3.3. PPATs mutated at three or four sites

PPAT(M2T/V70K/E212G) showed 1.2-fold lower catalytic efficiency for 2-oxoglutarate than that of PPAT(M2T/V70K) (Table 1), indicating that the additive mutation at Glu212 of PPAT(M2T/V70K) did not synergically increase the catalytic efficiency. PPAT(M2T/Y35H/V70K) showed 7.3-fold higher and 2.4-fold lower catalytic efficiency for 2-oxoglutarate than that of the wild-type PPAT and PPAT(Y35H/V70K), respectively. Thus, the additional mutation of Met2 of PPAT(Y35H/V70K) to Thr partially retarded the beneficial effect of the double mutation (Table 1). PPAT(Y35H/V70R/F247C) showed 6.2-fold higher catalytic efficiency for 2-oxoglutarate than that of PPAT(V70R/F247C); the Tyr35 substitution with His increased the affinity for 2-oxoglutarate. Thus, PPAT(Y35H/V70R/F247C) showed 39.8-fold higher catalytic efficiency for 2-oxoglutarate than that of the wild-type PPAT (Table 1). The catalytic efficiency increased by synergic effects on the affinity and the catalytic turnover for 2-oxoglutarate.

Relationship between catalytic turnover numbers of 2-oxoglutarate and pyruvate is shown in Fig. 3. They showed a negative correlation and a correlation coefficient was -0.96 ; as the values of k_{cat} of 2-oxoglutarate increase, those of pyruvate decrease. The results clearly showed that the in vitro mutation of PPAT successfully changed its substrate specificity.

The catalytic efficiency for L-glutamate of mutated PPATs with the high catalytic efficiency for 2-oxoglutarate was also determined. PPAT(Y35H/V70R/F247C), PPAT(Y35H/V70K), PPAT(M2T/Y35H/V70K), PPAT(M2T/Y35H/V70K/E212G), PPAT(V70R/F247C), and PPAT(V70K) showed 12.7-, 8.3-, 5.8-, 4.8-, 2.8-, and 1.6-fold higher catalytic efficiency for L-glutamate, respectively. Although the values were not the same as those for 2-oxoglutarate, the mutated PPATs, which had high catalytic efficiencies for 2-oxoglutarate, also showed high catalytic efficiencies for L-glutamate as well. The results coincided well with the fact that PPAT reaction is totally reversible [13], and showed that these mutated PPATs could be used for synthesis of pyridoxamine with L-glutamate as an amino donor.

3.4. Deduced mechanism of the enhanced catalytic efficiency of PPAT(Y35H/V70R/F247C)

The PPAT(Y35H/V70R/F247C) showed the highest reaction efficiency. Docking simulation was performed for pyridoxyl-L-glutamate to the model of the PPAT(Y35H/V70R/F247C) (Fig. 4).

Table 2
Location of residues mutated and resultant effect.

Original residue (new residue)	Location	Effect of substitution
Met 2 (Thr)	Surface	Increase in pyridoxamine production with cells
Tyr35(His)	Active site	Increase in reactivity toward 2-oxoglutarate
Val 70 (Lys)	Active site	Increase in reactivity toward 2-oxoglutarate
Val 70 (Arg)	Active site	Elimination of activity
Glu212 (Gly)	Surface	Increase in pyridoxamine production with cells
Phe247 (Cys)	Hydrophobic core	Reactivation of V70R mutated enzyme

The α -carboxyl group of the glutamate moiety is hydrogen-bonded to Arg345 and Tyr95. The γ -carboxyl group of the glutamate moiety is hydrogen-bonded to N ϵ of His35 with a distance of 2.9 Å rather than to Arg70, which has been predicted to be necessary for binding of the γ -carboxyl group of the glutamate moiety (Fig. 1B). The results were consistent with the high affinity of the PPAT(Y35H/V70R/F247C) for L-glutamate. The model was also in good agreement with the result that all mutated PPATs with His35 have high affinities towards L-glutamate (Table 1).

The location of residues whose substitution affected the reactivity of PPAT or productivity of pyridoxamine with cells is summarized in Table 2. Interestingly, the mutation of residues located on the surface of PPAT increased the productivity of pyridoxamine with *E. coli* cells expressing the mutated PPATs. The mutation of the residues located in the active site of PPAT affected the reactivity towards 2-oxoglutarate. The additional mutation of the residue located in a hydrophobic core reactivated the enzyme inactivated by the first mutation. The mechanism of the reactivation needs further studies.

3.5. Synthesis of pyridoxamine with L-glutamate as an amino donor by the intact *E. coli* cells expressing the mutated PPATs

Our purpose is to develop an industrial synthetic method of pyridoxamine with the recombinant *E. coli* cells expressing the mutated PPATs. Thus, in vitro synthesis of pyridoxamine was examined. The recombinant cells expressing the mutated PPATs could produce higher concentrations of pyridoxamine from pyridoxal and L-glutamate than those expressing the wild-type PPAT as shown in Table 1; although the expression levels of PPAT proteins examined by the SDS-PAGE were almost the same as shown in Fig. 2B. The cells expressing the quadruple mutated PPAT showed the best production of pyridoxamine, and could change 66 mM of pyridoxal in the reaction mixture to pyridoxamine in 48 h, when the production curve reached to a saturation level; because about 30 mM of pyridoxamine was produced in the control reaction by the well-known non-enzymatic transamination [17], it can

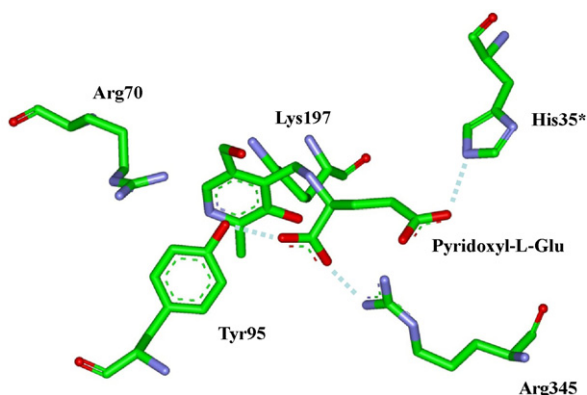


Fig. 4. A model of the active site of a complex of PPAT(Y35H/V70R/F247C) and pyridoxyl-L-glutamate. The asterisk means a residue of another subunit. The figures were drawn with WebLab.

be concluded that almost all pyridoxal was practically converted into pyridoxamine. PPAT(M2T/Y35H/V70K), PPAT(M2T/V70K), PPAT(M2T/V70K/E212G), and PPAT(Y35H/V70R/F247C) produced 40, 32, 31, and 27 mM of pyridoxamine, respectively. Interestingly, the order of the pyridoxamine production from the transformed *E. coli* cells did not correlate with the k_{cat} values of the mutated PPATs expressed in the *E. coli* cells; the correlation coefficient between the k_{cat} and the pyridoxamine production was -0.01 . The correlation coefficient between the catalytic efficiency and the pyridoxamine production was 0.13 showing no correlation between these values. In contrast, the correlation coefficient between K_m and the pyridoxamine production was -0.49 showing a low correlation between these values. Because K_m values are lower for enzymes with greater affinity, the mutated PPATs with higher affinity for 2-oxoglutarate converted pyridoxal into pyridoxamine with the highest efficiency in the *E. coli* cells. Thus, the increase in affinity for the substrate used as a starting material was more effective than the increase in k_{cat} for the bio-production with the transformed cells. The crowding environment in the intact bacterial cells could negate the beneficial effect of the increase in the k_{cat} and catalytic efficiency values [18] by an unknown reason.

4. Conclusion

In this study, the rational design and the random mutagenesis were used in combination to generate mutated PPATs with the high activity toward 2-oxoglutarate and L-glutamate. The transformed *E. coli* cells expressing PPAT(M2T/Y35H/V70K/E212G) could be used for in vitro conversion of pyridoxal into pyridoxamine with L-glutamate as an amino donor.

Acknowledgments

This work was supported in part by a Grant-in-Aid for a Research Fellowship from the Japan Society for the Promotion of Science for Young Scientists, and by a Kochi University President's Discretionary Grant.

References

- [1] R.A. John, *Biochim. Biophys. Acta* 1248 (1995) 81–96.
- [2] P. Bilski, M.Y. Li, M. Ehrenshaft, M.E. Daub, C.F. Chignell, *Photochem. Photobiol.* 71 (2000) 129–134.
- [3] H. Chen, L. Xiong, *Plant J.* 44 (2005) 396–408.
- [4] S.A. Denslow, A.A. Walls, M.E. Daub, *Physiol. Mol. Plant Pathol.* 66 (2005) 244–255.
- [5] M. Ehrenshaft, P. Bilski, M.Y. Li, C.F. Chignell, M.E. Daub, *Proc. Natl. Acad. Sci. U.S.A.* 96 (1999) 9374–9378.
- [6] R. Chumnantana, N. Yokochi, T. Yagi, *Biochim. Biophys. Acta* 1722 (2005) 84–91.
- [7] T.O. Metz, N.L. Alderson, S.R. Thorpe, J.W. Baynes, *Arch. Biochem. Biophys.* 419 (2003) 41–49.
- [8] P.A. Vozizyan, T.O. Metz, J.W. Baynes, B.G. Hudson, *J. Biol. Chem.* 277 (2002) 3397–3403.
- [9] T.P. Degenhardt, N.L. Alderson, D.D. Arrington, R.J. Beattie, J.M. Basgen, M.W. Steffes, S.R. Thorpe, J.W. Baynes, *Kidney Int.* 61 (2002) 939–950.
- [10] M.E. Williams, W.K. Bolton, R.G. Khalifah, T.P. Degenhardt, R.J. Schotzinger, J.B. McGill, *Am. J. Nephrol.* 27 (2007) 605–614.
- [11] M.V. Balyakina, N.L. Yakovleva, V.I. Gunar, *Pharm. Chem. J.* 14 (1980) 407–409.

- [12] R. Khalifah, R. Keilitz, C. Koellner, T.B. Degenhardt, R. Stephen, U.S. Patent 20,070,161,678 (2007).
- [13] Y. Yoshikane, N. Yokochi, K. Ohnishi, H. Hayashi, T. Yagi, *Biochem. J.* 396 (2006) 499–507.
- [14] Y. Yoshikane, N. Yokochi, M. Yamasaki, K. Mizutani, K. Ohnishi, B. Mikami, H. Hayashi, T. Yagi, *J. Biol. Chem.* 283 (2008) 1120–1127.
- [15] M.M. Bradford, *Anal. Biochem.* 72 (1976) 248–254.
- [16] S.C. Gill, P.H. Hoppel, *Anal. Biochem.* 182 (1989) 319–326.
- [17] D.E. Metzler, E.E. Snell, *J. Am. Chem. Soc.* 74 (1952) 979–983.
- [18] J.R. Ellis, *Trends Biochem. Sci.* 26 (2001) 597–604.